Molecular Biology of the Cell
Vol. 16, 5773–5783, December 2005

Plasma Membrane Organization Is Essential for Balancing Competing Pseudopod- and Uropod-promoting Signals during Neutrophil Polarization and Migration [D] [V]

Stéphane Bodin and Matthew D. Welch

Department of Molecular and Cell Biology, University of California, Berkeley, CA 94720

Submitted April 28, 2005; Revised September 24, 2005; Accepted September 26, 2005
Monitoring Editor: Clare Waterman-Storer

Exposure of neutrophils to chemoattractant induces cell polarization and migration. These behaviors require the asymmetric activation of distinct signaling pathways and cytoskeletal elements in the protruding pseudopod at the front of cells and the retracting uropod at the rear. An important outstanding question is, how does the organization of the plasma membrane participate in establishing asymmetry during polarization and migration? To answer this question, we investigated the function of cholesterol, a lipid known to influence membrane organization. Using controlled cholesterol depletion, we found that a cholesterol-dependent membrane organization enabled cell polarization and migration by promoting uropod function and suppressing ectopic pseudopod formation. At a mechanistic level, we showed that cholesterol was directly required for suppressing inappropriate activation of the pseudopod-promoting G_i/PI3-kinase signaling pathway. Furthermore, cholesterol was required for dampening G_i-dependent negative feedback on the RhoA signaling pathway, thus enabling RhoA activation and uropod function. Our findings suggest a model in which a cholesterol-dependent membrane organization plays an essential role in the establishment of cellular asymmetry by balancing the activation and segregating the localization of competing pseudopod- and uropod-inducing signaling pathways during neutrophil polarization and migration.

INTRODUCTION

A variety of cells respond to a gradient of chemoattractant by migrating up the gradient toward the source of the attractant, a behavior called chemotaxis. For example, neutrophils undergo directional migration toward chemokines and bacterial peptides that mark sites of inflammation and infection. Neutrophils can also respond to uniform concentrations of chemoattractant by migrating in a random direction, a behavior called chemokinesis. During chemotaxis and chemokinesis, directional migration depends on the acquisition of a polarized morphology and the establishment of functionally distinct front and rear structures, which in neutrophils are called the pseudopod and the uropod, respectively. Migration involves pseudopod protrusion driven by actin filament polymerization at the leading edge (Wallace *et al.,* 1984) and uropod retraction powered by contractile activities of actin and myosins at the rear (Niggli, 1999; Eddy *et al.,* 2000; Xu *et al.,* 2003).

For neutrophils or neutrophil-like HL-60 cells to polarize and migrate in response to the chemoattractant f-Met-Leu-Phe (fMLP), distinct signaling pathways must be activated at the front and the rear of the cell. At the front, pseudopod formation requires the activation of the heterotrimeric GTP-binding protein G_i (Shefcyk *et al.,* 1985) as well as the subsequent activation of the Rho family GTPase Rac (Benard *et al.,* 1999; Srinivasan *et al.,* 2003). Cell polarization and efficient chemotaxis also require the activation of phosphoinositide 3-kinases (PI3-Ks) (Niggli and Keller, 1997; Li *et al.,* 2000; Sasaki *et al.,* 2000) and the synthesis of the D3-phosphoinositide lipid products (D3-PIs), phosphatidylinositol (3,4,5) *Tris*-phosphate (PI(3,4,5)P_3) and phosphatidylinositol (3,4) *bis*-phosphate (PI(3,4)P_2), which concentrate at the leading edge (Servant *et al.,* 2000). These D3-PIs serve as docking sites for pleckstrin homology (PH)-domain containing proteins, such as protein kinase B (Akt; Servant *et al.,* 2000) and the Rac guanine nucleotide exchange factor (GEF) P-Rex1 (Welch *et al.,* 2002). D3-PIs activate Rac in a positive feedback loop, promoting actin polymerization at the leading edge (Niggli, 2000; Wang *et al.,* 2002; Weiner *et al.,* 2002). Many features of this frontness pathway are conserved in the evolutionarily distant organism *Dictyostelium discoideum* (Parent, 2004). At the rear of neutrophils, uropod formation requires the activation of the heterotrimeric GTP-binding protein $G_{12/13}$ (Xu *et al.,* 2003) and the downstream activation of the Rho family GTPase RhoA, as well as the kinases Rho-kinase (ROCK; Alblas *et al.,* 2001) and myosin light chain kinase (MLC-K; Xu *et al.,* 2003). This pathway stimulates the recruitment and activation of myosin II, which is critical for uropod formation and retraction (Eddy *et al.,* 2000; Xu *et al.,* 2003).

Although it is clear that these signaling pathways are spatially localized at the front and rear, the mechanisms by which this polarization is established and maintained remain poorly understood. Polarization may involve the activity of a mutual negative feedback system that inhibits the rear pathway from being activated at the front and vice versa (Xu *et al.,* 2003). This may be enhanced by self-organizing properties of the cytoskeleton, which would favor the

This article was published online ahead of print in *MBC in Press* (http://www.molbiolcell.org/cgi/doi/10.1091/mbc.E05–04–0358) on October 5, 2005.

[D] [V] The online version of this article contains supplemental material at *MBC Online* (http://www.molbiolcell.org).

Address correspondence to: Matthew Welch (welch@berkeley.edu) or Stéphane Bodin (stbodin@uclink.berkeley.edu).

segregation of functionally incompatible cytoskeletal assemblies to opposite poles of the cell (Wang *et al.*, 2002; Xu *et al.*, 2003).

Another intriguing mechanism for polarization may involve the compartmentalization of the plasma membrane itself. This concept is supported by an emerging model, distinct from the classical fluid mosaic model (Singer and Nicolson, 1972), which suggests that the plasma membrane is organized into discrete domains of various sizes with different lipid and protein compositions (Edidin, 2003; Zurzolo *et al.*, 2003). Distinct plasma membrane domains in the pseudopod and uropod may be crucial for establishing and maintaining an asymmetrical distribution of signaling pathways and cytoskeletal elements in these two structures.

Cholesterol is one component of the plasma membrane that plays a critical role in the formation of membrane domains. In some cells, cholesterol is enriched in discrete areas of the plasma membrane (Gatfield and Pieters, 2000; Millan *et al.*, 2002; Pardo and Nurse, 2003; Vasanji *et al.*, 2004). It is known to influence the lateral assembly of phospholipids into microdomains in vitro (Xu and London, 2000; Dietrich *et al.*, 2001), and in cells it is a major component of lipid rafts, which are domains where specific lipids and proteins assemble into complexes involved in signal transduction (Zurzolo *et al.*, 2003). In migrating neutrophils, lipid raft markers exhibit a polarized distribution and have been observed either exclusively in the uropod (Seveau *et al.*, 2001) or in distinct populations in the pseudopod and uropod (Gomez-Mouton *et al.*, 2004). Moreover, depletion of plasma membrane cholesterol has been found to cause a complete inhibition of neutrophil and HL-60 cell polarization and migration responses (Seveau *et al.*, 2001; Pierini *et al.*, 2003; Gomez-Mouton *et al.*, 2004; Niggli *et al.*, 2004). Cholesterol depletion also inhibits signaling via mitogen-activated protein kinase and protein kinase C (Niggli *et al.*, 2004) and prevents sustained activation of Rac (Pierini *et al.*, 2003). Nevertheless, it is still not clear what function cholesterol-dependent membrane organization plays in pseudopod and uropod formation or in the capacity of cells to activate different signaling pathways at opposite poles during polarization and migration.

By employing controlled cholesterol depletion conditions that do not abolish cell responsiveness, we dissect the mechanism by which cholesterol-dependent membrane organization participates in polarization and migration. We find that cholesterol is required to maintain a balance between competing pseudopod- and uropod-promoting signals. In particular, cholesterol is critical to promote the function and stabilization of the uropod and to limit pseudopod formation to a single membrane area. At the molecular level, cholesterol is essential for local activation of the RhoA pathway and for suppressing ectopic G_i/PI3-K activation and restricting sites of D3-PI accumulation. Thus, cholesterol is essential for organizing the plasma membrane into domains that enable local activation of signaling pathways and cytoskeletal elements during neutrophil chemotaxis and chemokinesis.

MATERIALS AND METHODS

Reagents, Antibodies, and Cell Lines

fMLP, methyl-β-cyclodextrin (MβCD), pertussis toxin, HRP-conjugated cholera toxin-B, and wortmannin were from Sigma (St. Louis, MO). Rhodamine-phalloidin and Alexa Fluor 488-phalloidin were from Molecular Probes (Eugene, OR). ^{3}H-labeled cholesterol was from Amersham Biosciences (Piscataway, NJ). Anti-RhoA, anti-CD71, and anti-Fyn antibodies were from Santa Cruz Biotechnology (Santa Cruz, CA). Anti-phospho(Ser473)-Akt and anti-Akt antibodies were from Cell Signaling Technology (Beverly, MA). Anti-$G_{i\alpha1-2}$ antibody was from Upstate Cell Signaling (Waltham, MA). Anti-P-Rex1 antibody was a gift from Dr. H. C. Welch (Babraham Institute, Cambridge, United Kingdom). FITC-conjugated secondary antibodies were from Jackson ImmunoResearch (West Grove, PA). HL-60 cells stably expressing PH-Akt-GFP were a gift from Dr. H. R. Bourne (University of California, San Francisco, San Francisco, CA).

Cell Culture, Chemokinesis, and Micropipette Chemotaxis Assays

HL-60 cells were maintained in RPMI 1640 with 25 mM HEPES, 10% fetal bovine serum (FBS) and penicillin/streptomycin (RPMI-HEPES) and were differentiated into neutrophil-like cells by incubation with 1.3% dimethyl sulfoxide for 5–7 d. For chemotaxis and chemokinesis assays, dHL-60 cells were plated onto fibronectin-coated coverslips (5 $\mu g/cm^2$), incubated for 3 min with or without 2.5 mM MβCD in modified Hanks' balanced salt solution (mHBSS), washed, and incubated for 5 min in MβCD-free mHBSS before stimulation. For chemokinesis assays, cells were stimulated uniformly by fMLP (100 nM). For chemotaxis assays, cells were exposed to a chemoattractant gradient diffusing from a micropipette filled with fMLP (5 μM).

Measuring Cholesterol Depletion

dHL-60 cells at 1×10^6 cells/ml in RPMI-HEPES, 10% FBS, penicillin/streptomycin were incubated for 8 h at 37°C in the presence of ^{3}H-labeled cholesterol (8 Ci/mmol, 6.25 μCi/ml), washed with phosphate-buffered saline (PBS), and placed in culture media for 20 h at 37°C to allow ^{3}H-labeled cholesterol to equilibrate with the cellular pool. Cells were then incubated with increasing concentrations of MβCD for different times. After centrifugation to isolate cells, the level of cholesterol depletion was determined by quantifying the radioactivity in the pellet and supernatant by liquid scintillation counting. Each fraction was subjected to lipid extraction as described in Bodin *et al.* (2001), which confirmed that 96 ± 2% of the radioactivity was associated with cholesterol.

Microscopy

Fixation of cells was carried out in PBS with 3.7% paraformaldehyde for 15 min. Cells were permeabilized with PBS with 0.1% Triton X-100 for 1 min. RhoA and P-Rex1 were visualized by indirect immunofluorescence using standard protocols (Welch *et al.*, 2002). F-actin was stained with rhodamine-phalloidin (5 U/ml, 5 min). Live cell imaging was carried out at 37°C in mHBSS using an Olympus IX71 microscope (Melville, NY). Images were captured using a Photometrics CoolSnap HQ camera (Tucson, AZ) and Metamorph software (Universal Imaging, West Chester, PA), and were edited using Photoshop (Adobe Systems, San Jose, CA).

Isolation of Detergent-resistant Membranes

Detergent-resistant membranes (DRMs) were isolated as described in (Drevot *et al.*, 2002). Briefly, dHL-60 cells (2×10^8 cells) treated with or without MβCD (2.5 mM, 3 min) were resuspended in 1 ml buffer A (25 mM HEPES pH 7.2, 150 mM NaCl, 1 mM EGTA, 5 mM DFP, 1 mM Na_3VO_4, 1 mM phenylmethylsulfonyl fluoride [PMSF], 10 μg/ml LPC). Cells were then sonicated on ice (3×, 10 s each) and centrifuged (800 × *g*, 5 min, 4°C). The supernatant was supplemented with Brij98 (1%, 5 min, 37°C) and mixed with prewarmed buffer A containing 2.74 M sucrose. This mix was placed at the bottom of a sucrose step gradient (1—0.8—0.6— 0.5—0.3—0.15 M) and centrifuged (200,000 × *g*, 16 h, 4°C). Fractions were harvested from the top of the gradient, and 20 μl of each fraction was spotted onto a nitrocellulose membrane to determine GM1-distribution by dot blot as described previously (Ilangumaran and Hoessli, 1998). The distribution of Fyn, $G_{\alpha i}$, and CD71 across the gradient was determined by Western blot as described previously (Bodin *et al.*, 2001).

RhoA-GTP Pulldown Assays

RhoA-GTP pulldown assays were performed as described previously (Ren *et al.*, 1999). The plasmid encoding GST-RBD (RhoA-binding domain of human Rhotekin fused to GST) was a gift of Dr. G. S. Martin. The GST-RBD protein was purified from *Escherichia coli* as described previously (Ren *et al.*, 1999). dHL-60 cells (1×10^6 cells/ml) were incubated in the presence or absence of MβCD (2.5 mM, 3 min), washed, and resuspended in mHBSS (1 ml, 2×10^7 cells/ml), and stimulated by fMLP (1 μM, 1 min). Cells were resuspended in 500 μl of ice-cold buffer G (50 mM Tris, pH 7.5, 150 mM NaCl, 10 mM $MgCl_2$, 0.9% Triton X-100, 5 mM DFP, 2.5 mM EGTA, 1 mM Na_3VO_4, 1 mM PMSF, 10 μg/ml LPC). Lysates were passed five times through a 27-gauge needle and centrifuged (800 × *g*, 10 min, 4°C). Five percent of the supernatant was taken for an input control. GST-RBD, 50 μg, on glutathione Sepharose beads (Amersham) was incubated with the remaining supernatant for 1 h at 4°C. Beads were washed twice in buffer G and once in buffer G without Triton X-100. RhoA-GTP was visualized by SDS-PAGE and Western blotting using anti-RhoA antibody and quantified by densitometry using NIH Image software.

Measurement of Akt Phosphorylation

dHL-60 cells were resuspended in RPMI-HEPES (1×10^6 cells/ml) and incubated with or without MβCD (2.5 mM, 3 min). For inhibitor treatments, cells were preincubated with PTX (1 μg/ml, overnight) or wortmannin (70 nM, 2 h). Cells were washed, resuspended in mHBSS (1×10^6/ml, 5 min, 37°C) and stimulated by fMLP (1 μM, 1 min). Stimulation was stopped by centrifugation (14,000 $\times$ *g*, 15 s, 4°C) and lysis in SDS-PAGE sample buffer. Phosphorylation of Akt was visualized by Western blotting using anti-phospho-Ser473-Akt antibody and quantified by densitometry using NIH Image software. Membranes were stripped and reprobed with anti-Akt antibody for an input control.

RESULTS

Moderate Cholesterol Depletion from dHL-60 Cells

To study the role of plasma membrane cholesterol in differentiated HL-60 (dHL-60) cell polarization and migration, we performed cholesterol depletion using MβCD (Klein *et al.*, 1995). Previous studies have shown that MβCD treatments resulting in >90% depletion induce side effects such as calcium-influx and membrane depolarization (Bodin *et al.*, 2001; Gousset *et al.*, 2002; Pizzo *et al.*, 2002). In contrast, more moderate treatments resulting in 60–70% depletion specifically alter signal transduction processes without producing side effects on cell physiology (Bodin *et al.*, 2001; Pizzo *et al.*, 2002). To set up moderate depletion conditions for dHL-60 cells, we systematically measured the depletion of ^{3}H-labeled cholesterol after incubation with several concentrations of MβCD for different times (Supplementary Material, Supplementary Figure S1). We achieved a modest 67 $\pm$ 5% depletion after a 3-min incubation with 2.5 mM MβCD (Supplementary Material, Supplementary Figure S1). Under these conditions, no effect on viability, adherence to fibronectin or the basal level of cytosolic Ca^{2+} was detected (unpublished data).

To examine the effect of depletion on cholesterol function, we tested for disruption of the integrity of cholesterol-rich raft domains (Simons and Ikonen, 1997). Rafts from control cells were isolated as DRMs that cofractionated with the marker molecules ganglioside GM1 and Fyn in the light density fractions of a sucrose gradient (Supplementary Material, Supplementary Figure S1; Ilangumaran *et al.*, 1998; Drevot *et al.*, 2002). By contrast, in MβCD-treated cells, GM1 and Fyn were shifted toward the heavy fractions, indicating that raft integrity was disrupted. We concluded that moderate cholesterol depletion disrupted cholesterol-dependent membrane organization without dramatically affecting cell physiology.

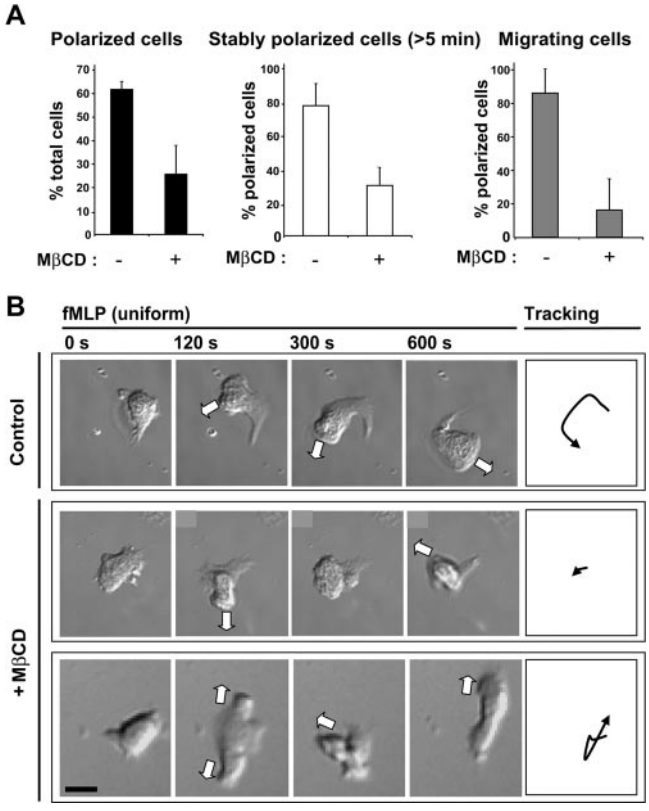

Figure 1. Controlled cholesterol depletion disturbs polarization and migration induced by uniform fMLP-stimulation. (A) Graphs showing: (left) the percentage of control and MβCD-treated cells able to polarize upon stimulation with fMLP (100 nM, 14 min); middle, the percentage of polarized control or MβCD-treated cells able to maintain their polarity for at least 5 min; right, the percentage of polarized control and MβCD-treated cells that undergo migration over a 10-min time course. Results are means $\pm$ SD for four separate experiments (n = 126 control cells and n = 146 cholesterol-depleted cells). (B) Time-lapse DIC images of individual cells stimulated with fMLP. Top row, a stably polarized control cell; middle and bottom rows, MβCD-treated cells forming multiple protrusions, either successively (middle) or simultaneously (bottom). The white arrows indicate the directions of the protrusions. Right, trajectories of the center of each cell. Scale bar, 10 μm.

Cholesterol Is Required for Polarization and Migration

We investigated the effects of cholesterol depletion on the ability of dHL-60 cells to polarize and migrate, either in response to a uniform fMLP concentration or to an fMLP gradient. Cells were first depleted of cholesterol using the conditions described above and then immediately placed into fresh MβCD-free media. The behavior of cells was observed using time-lapse DIC microscopy. On uniform fMLP stimulation, most control cells adopted a polarized morphology characterized by the development of a single pseudopod and uropod, and the majority maintained their polarity for more than 5 min (Figure 1A). In contrast, significantly fewer cholesterol-depleted cells established a clear polarity, and most of these cells were unable to maintain their polarized morphology over a similar time period. Among the population of cholesterol-depleted cells that were able to polarize, the percentage of cells able to migrate was reduced fivefold. The majority of MβCD-treated cells responded to fMLP-stimulation by emitting several protruding pseudopods, either successively or simultaneously (Figure 1B). Thus, a cholesterol-dependent membrane organization is critical for polarization and chemokinesis in response to uniform fMLP stimulation.

To observe polarization and migration of individual cells in response to a gradient of fMLP, we examined the behavior of dHL-60 cells exposed to fMLP flowing from a micropipette. Compared with control cells, significantly fewer MβCD-treated cells polarized and migrated, and migration velocity was reduced fourfold (Figure 2, A and B; Supplementary Material, Supplementary Video 1). The migration defect was not due to an inability to sense the chemoattractant gradient, because the majority (92%, n = 25) of cholesterol-depleted cells polarized and developed a single pseudopod facing a pipette tip that was positioned a short distance away (5–10 μm). We also reversed the order of events and exposed cells to an fMLP-gradient before transiently treating them with MβCD for 3 min. Under these conditions, ~1 min after the end of MβCD treatment, cells began to exhibit a dramatic decrease in velocity (Figure 2C).

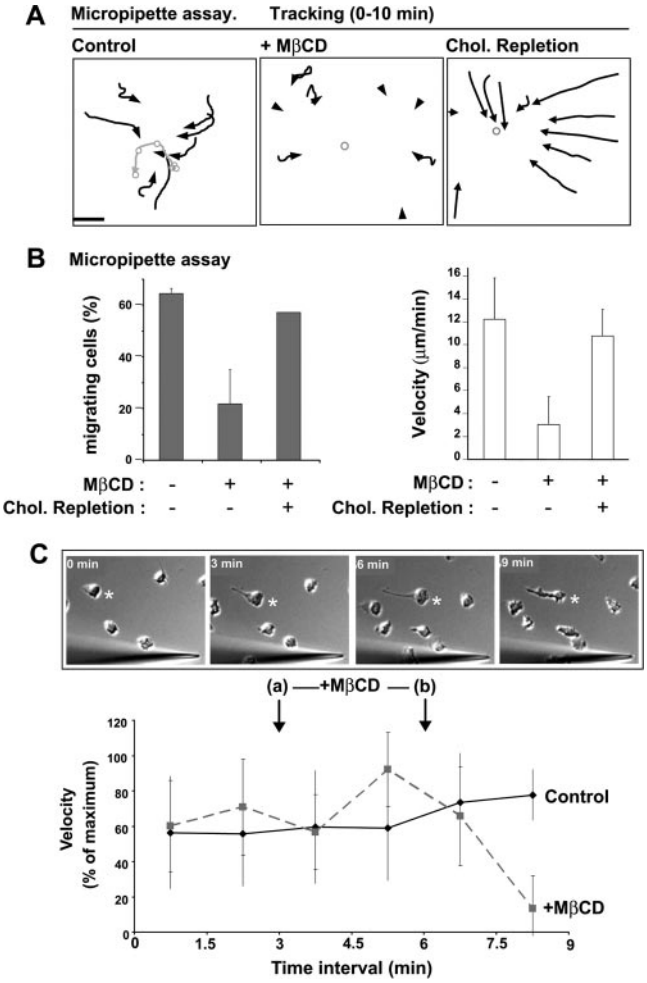

Figure 2. Cholesterol depletion inhibits the chemotaxis response. (A) Cell trajectories (black arrows) over a 10-min time course for control, MβCD-treated, or MβCD-treated and cholesterol-replenished cells stimulated with an fMLP-gradient diffusing from a micropipette (Supplementary Video 1). The gray circle/line indicates the positions of the micropipette. Data are representative of 2–5 separate experiments. Scale bar, 50 μm. (B) Graphs representing the percentage of cells able to migrate (left), and migration velocity (right) for control, MβCD-treated, or MβCD-treated and cholesterol-replenished cells stimulated for 10 min by an fMLP gradient diffusing from a micropipette. Data are mean ± SD for 2–3 independent experiments. (C) Effect of treating cells with MβCD after polarization in response to an fMLP-gradient. At t = 3 min (a), MβCD-free media was replaced with the same media or media containing MβCD (2.5 mM). At t = 6 min (b), media was replaced again with MβCD-free media. (Bottom) Graph showing the average velocity of control and MβCD-treated cells at time intervals of 1.5 min. Results are expressed as percentage of the maximum speed (mean ± SD, 3 independent experiments). Top, time-lapse DIC images of a representative migrating cell (asterisk) that exhibits a collapse in polarity 1 min after the end of MβCD treatment. Scale bar, 10 μm.

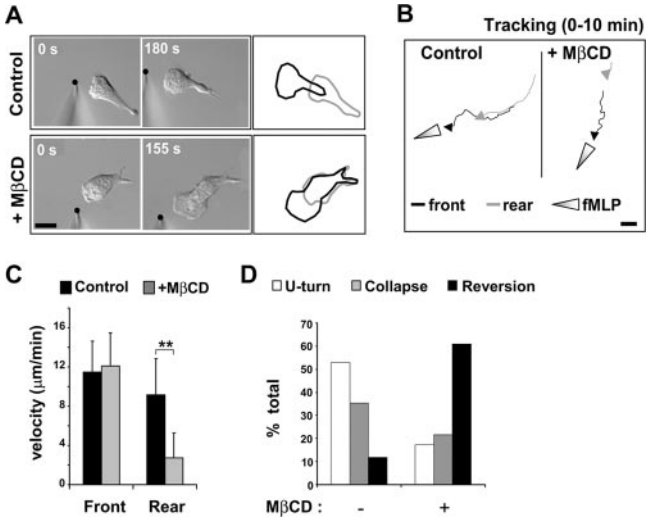

Figure 3. Cholesterol is required for the function of the uropod. (A) DIC images of control and MβCD-treated dHL-60 cells responding to a point source of fMLP (black dot). Outlines of the cells at the start (gray) and the end (black) of the time course reveal the migration response. (B) Tracking analysis of the front and rear edges of a control cell and an MβCD-treated cell stimulated with an fMLP-gradient for 10 min. Scale bar, 10 μm. (C) Quantification of the velocity of the front and rear edges of control and MβCD-treated cells. Results are expressed as mean ± SD for three independent experiments (n = 21 for control cells, n = 18 MβCD-treated cells). Differences between front and rear velocity were statistically significant according to the Student's *t*-test (** $p < 0.01$). (D) Graph representing the percentage of cells that display a U-turn, a collapse of polarity, or a reversion of polarity after a sudden inversion of the chemoattractant gradient (n = 17 control cells and n = 23 for MβCD-treated cells in 3 separate experiments; see also Supplementary Figure S2 and Supplementary Video 2).

The pseudopod of most cells dissolved and ruffling activity was apparent around the entire periphery (Figure 2C). The effects of cholesterol-depletion were reversible, because MβCD-treated cells that were allowed to replenish cholesterol in MβCD-free media as described previously (Friedrichson and Kurzchalia, 1998; Niggli *et al.*, 2004) exhibited a normal chemotaxis response (Figure 2, A and B). Thus, cholesterol is critical for the establishment and maintenance of cell polarization and migration under chemotaxis and chemokinesis conditions.

Cholesterol Is Specifically Required for the Function of the Uropod

To determine the cause of the defect in cell migration, we performed separate tracking analyses of the trajectories of the leading and rear edges of single cells stimulated by a point source of fMLP (Figure 3A). MβCD-treated cells showed a significantly reduced rear-edge velocity compared with control cells (Figure 3, A–C). Remarkably, the velocity of the leading edge was unaffected, although its continuous forward movement was altered, probably because of the resistance applied by the slow moving rear edge. Thus, the inhibition of chemotaxis in cholesterol-depleted cells was due to a specific inhibition of uropod retraction, not of pseudopod protrusion.

The specificity of the rear edge retraction defect led us to examine the stability of the uropod in MβCD-treated cells. In control polarized neutrophils and dHL-60 cells, the attractant sensitivity of the uropod is strongly inhibited (Zigmond *et al.*, 1981; Xu *et al.*, 2003). As a consequence, if cells are induced to polarize and migrate toward a micropipette tip emitting fMLP, and then are suddenly subjected to a gradient inversion by repositioning the fMLP point source near their rear, the majority respond by maintaining their polarity and executing a U-turn, or by collapsing their polarity (Zigmond *et al.*, 1981; Supplementary Material, Supplementary Figure S2). Very few cells reverse their polarity

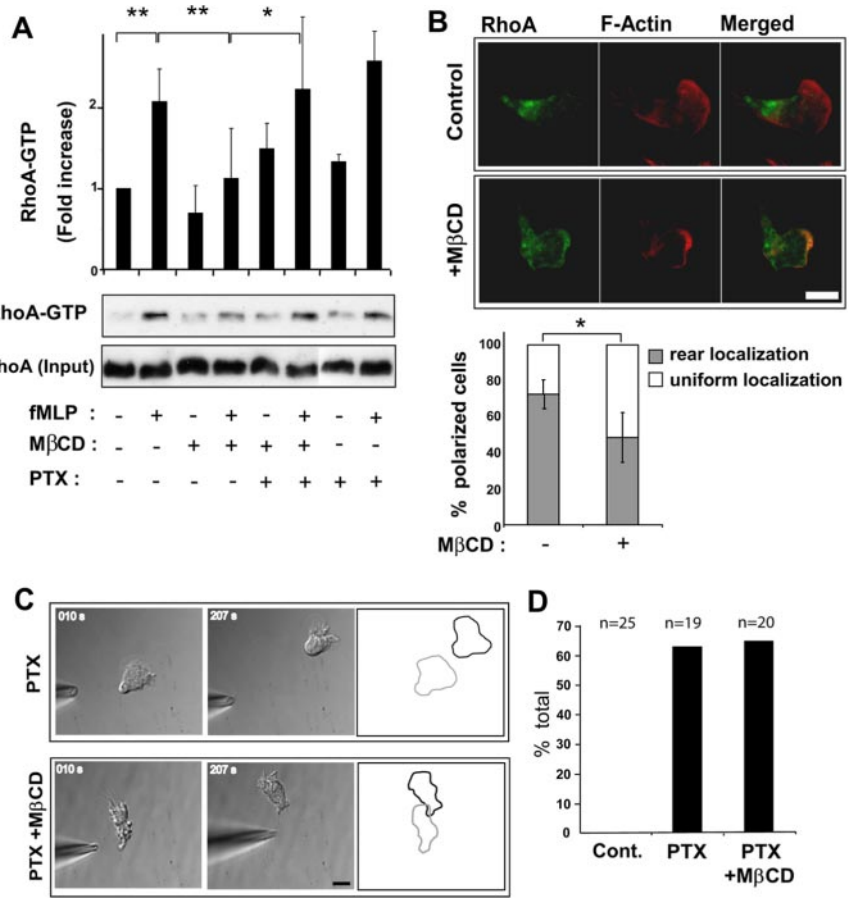

Figure 4. Cholesterol facilitates RhoA activation indirectly through an effect on the G_i pathway. (A) Measurement of RhoA-GTP levels in control dHL-60 cells, MβCD-treated cells, MβCD-treated and pertussis toxin (PTX; 1 μg/ml, overnight)-treated cells and PTX-treated cells after stimulation with uniform fMLP, monitored by GST-Rhotekin-RBD pulldowns and Western blotting. The graph represents a quantification of densitometry results expressed as fold increase in RhoA-GTP compared with resting conditions (mean ± SD, 3–5 separate experiments). Differences between fMLP-treated versus resting control cells, fMLP- versus fMLP/MβCD-treated cells (** $p < 0.01$) and fMLP/MβCD- versus fMLP/PTX/MβCD-treated cells (* $p < 0.05$) were statistically significant according to the Student's *t*-test. (B) Fluorescence images of RhoA and F-actin in a control and MβCD-treated cell stimulated with uniform fMLP (100 nM, 2 min). Scale bar, 10 μm. The graph represents the percentage of polarized cells exhibiting rear or uniform RhoA distribution. Results are expressed as mean ± SD for three experiments (n = 182 control cells and n = 184 MβCD-treated cells). Differences between control and MβCD-treated cells were statistically significant according to the Student's *t*-test (* $p < 0.05$). (B) Time-lapse DIC images of fMLP-induced uropod formation in PTX- or PTX/MβCD-treated dHL-60 cells. Cell outlines represent the starting (gray) and the ending (black) positions of the cell during the time course. Scale bar, 10 μm. (D) Graph representing the percentage of control (cont.), PTX-treated cells and PTX/MβCD-treated cells that formed a retracting uropod facing the pipette tip.

and form a pseudopod at the rear. Using this gradient inversion method, we investigated the stability and chemoattractant sensitivity of the uropod in cholesterol-depleted cells. Unlike control cells, the majority of MβCD-treated cells reversed their polarity upon gradient inversion and emitted a new pseudopod from their rear (Figure 3D; Supplementary Material, Supplementary Figure S2 and Supplementary Video 2). These observations indicate that the presence of cholesterol in the plasma membrane is critical for multiple aspects of uropod function, including retraction and suppression of attractant sensitivity.

Cholesterol Acts Indirectly in the Activation of RhoA via a G_i-dependent Pathway

The defects caused by cholesterol depletion, which include inhibition of uropod formation and function, resemble the defects caused by inactivation of the $G_{12/13}$/RhoA pathway and downstream effectors such as ROCK, MLC-K, and myosin II (Eddy *et al.*, 2000; Xu *et al.*, 2003). Therefore, we measured the effect of MβCD-treatment on fMLP-induced RhoA activation by pulldown experiments using a fusion protein of GST and the Rho-binding domain of Rhotekin, which preferentially interacts with GTP-bound RhoA (Ren *et al.*, 1999). Compared with control cells, cholesterol-depleted cells exhibited a significant decrease in fMLP-induced RhoA-GTP (Figure 4A). The localization of RhoA was also disrupted in cholesterol-depleted cells stimulated with uniform fMLP. Although most polarized control cells displayed RhoA localization at their rear (Xu *et al.*, 2003; Li *et al.*, 2005), most polarized cholesterol-depleted cells displayed a uniform RhoA distribution (Figure 4B). Thus, the impairment of uropod function caused by cholesterol depletion is correlated with decreased RhoA activity and aberrant RhoA localization.

This observed inhibition of the RhoA pathway may reflect a direct role for cholesterol in RhoA regulation. Alternatively, it may reflect an indirect role for cholesterol in RhoA regulation if cholesterol instead functions to modulate the G_i/PI3-K/Rac signaling pathway, which is known to influence the RhoA pathway through negative feedback mechanism (Xu *et al.*, 2003). To discriminate between these possibilities, we investigated whether the ability of cholesterol depletion to inhibit RhoA activity was dependent on the activation of the G_i pathway. Cells were treated with the G_i-inhibitor pertussis toxin (PTX) and then incubated in the absence or presence of MβCD. The activation of RhoA was first investigated using pulldown assays, as described above. In contrast to cells treated only with MβCD, which showed reduced levels of activated RhoA, cells treated with both PTX and MβCD (or PTX alone) showed normal levels of activated RhoA in response to fMLP (Figure 4A). The function of RhoA in cells was next investigated by subjecting PTX/MβCD- and PTX-treated cells to a micropipette chemotaxis assay. As described previously (Xu *et al.*, 2003), most PTX-treated cells developed a retracting uropod instead of a pseudopod at their up-gradient edge (Figure 4, C and D; Supplementary Material, Supplementary Video 3). This uropod retraction response was prevented by directly blocking the RhoA pathway using the ROCK inhibitor Y-27632 (unpublished data), but it was not prevented by MβCD treat-

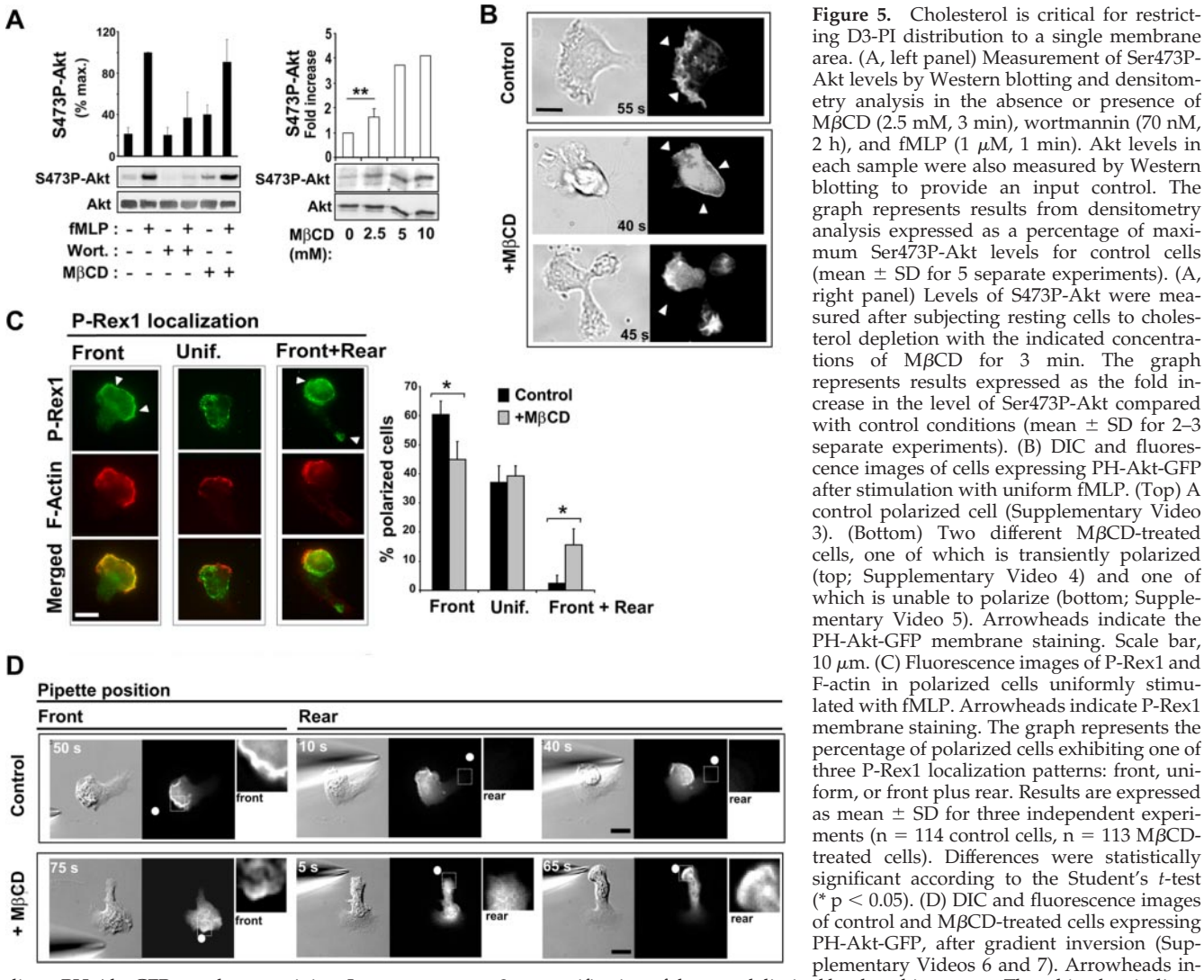

Figure 5. Cholesterol is critical for restricting D3-PI distribution to a single membrane area. (A, left panel) Measurement of Ser473P-Akt levels by Western blotting and densitometry analysis in the absence or presence of MβCD (2.5 mM, 3 min), wortmannin (70 nM, 2 h), and fMLP (1 μM, 1 min). Akt levels in each sample were also measured by Western blotting to provide an input control. The graph represents results from densitometry analysis expressed as a percentage of maximum Ser473P-Akt levels for control cells (mean $\pm$ SD for 5 separate experiments). (A, right panel) Levels of S473P-Akt were measured after subjecting resting cells to cholesterol depletion with the indicated concentrations of MβCD for 3 min. The graph represents results expressed as the fold increase in the level of Ser473P-Akt compared with control conditions (mean $\pm$ SD for 2–3 separate experiments). (B) DIC and fluorescence images of cells expressing PH-Akt-GFP after stimulation with uniform fMLP. (Top) A control polarized cell (Supplementary Video 3). (Bottom) Two different MβCD-treated cells, one of which is transiently polarized (top; Supplementary Video 4) and one of which is unable to polarize (bottom; Supplementary Video 5). Arrowheads indicate the PH-Akt-GFP membrane staining. Scale bar, 10 μm. (C) Fluorescence images of P-Rex1 and F-actin in polarized cells uniformly stimulated with fMLP. Arrowheads indicate P-Rex1 membrane staining. The graph represents the percentage of polarized cells exhibiting one of three P-Rex1 localization patterns: front, uniform, or front plus rear. Results are expressed as mean $\pm$ SD for three independent experiments (n = 114 control cells, n = 113 MβCD-treated cells). Differences were statistically significant according to the Student's *t*-test (* $p < 0.05$). (D) DIC and fluorescence images of control and MβCD-treated cells expressing PH-Akt-GFP, after gradient inversion (Supplementary Videos 6 and 7). Arrowheads indicate PH-Akt-GFP membrane staining. Insets represent a 3$\times$ magnification of the area delimited by the white square. The white dots indicate the position of the micropipette tip. Scale bar, 10 μm.

ment (Figure 4, C and D; Supplementary Material, Supplementary Video 3). In fact, the uropod retraction velocity of cells treated with both MβCD and PTX was similar to control cells treated with PTX only (unpublished data). These data indicate that membrane cholesterol does not directly affect the activity of RhoA or its downstream effectors, but rather indirectly influences RhoA activity via an effect on the G_i/PI3-K/Rac pathway.

Cholesterol Is Critical for Restricting D3-PI Synthesis to the Pseudopod during Self-polarization and Gradient Inversion

The results described above suggest that the role of a cholesterol-dependent membrane organization in polarization and migration is to modulate the G_i/PI3-K/Rac pathway, which is normally active only in the pseudopod and is important for the establishment and maintenance of polarity (Wang *et al.*, 2002; Weiner *et al.*, 2002). We therefore analyzed the effect of MβCD-treatment on PI3-K activation and the timing and location of D3-PI synthesis (Figure 5). Activation of PI3-K was observed indirectly by measuring the increase in phosphorylation of Akt on Ser473 (S473P-Akt; Figure 5A). Interestingly, treatment of resting cells with MβCD alone caused a dose-dependent increase in S473P-Akt relative to control levels (Figure 5A), suggesting that cholesterol is important for dampening PI3-K activation in the absence of fMLP. However, upon fMLP stimulation, control and cholesterol-depleted cells exhibited similar increases in S473P-Akt (Figure 5A).

Next, we observed whether the localized accumulation of D3-PIs and their effectors was disrupted by cholesterol depletion under chemokinesis conditions. To localize D3-PIs, we used dHL-60 cells that stably express a probe consisting of the PH domain of Akt, which binds D3-PIs, fused to GFP (PH-Akt-GFP; Servant *et al.*, 2000). In resting cells, PH-Akt-GFP was predominantly localized in the cytoplasm. On uniform fMLP-stimulation, PH-Akt-GFP in control and cholesterol-depleted cells translocated to the plasma membrane with similar kinetics, reflecting D3-PI synthesis. However, in contrast to polarized control cells, where the probe was localized at the leading edge of the pseudopod (Figure 5B; Supplementary Material, Supplementary Video 4; Servant *et al.*, 2000), polarized cholesterol-depleted cells exhibited staining that was uniformly distributed over the cell surface

(Figure 5B; Supplementary Material, Supplementary Video 5). In cholesterol-depleted cells that did not polarize but instead formed multiple protrusions, PH-Akt-GFP was localized to each protrusion (Figure 5B; Supplementary Material, Supplementary Video 6). The localization of the D3-PI effector P-Rex1, a PI(3,4,5)P_3-binding guanine nucleotide-exchange factor (GEF) for Rac (Welch *et al.,* 2002), was also affected by cholesterol depletion. In control polarized cells responding to uniform fMLP, P-Rex1 was primarily localized to the pseudopod or was uniformly distributed (Figure 5C). In contrast, P-Rex1 was also concentrated at the rear in a significant fraction of polarized cholesterol-depleted cells (Figure 5C), particularly those with an elongated trailing edge. Together these observations indicate that, in chemokinesis conditions, a cholesterol-dependent membrane organization is essential for restricting the localization of D3-PIs and their effectors to a single area of the membrane, offering a molecular correlation for the critical role of cholesterol in self-polarization.

Additionally, we examined whether cholesterol depletion affected the localized accumulation of D3-PIs in cells stimulated under chemotaxis conditions. In agreement with the fact that cholesterol depletion did not interfere with pseudopod formation under these conditions, both control and cholesterol-depleted cells exhibited PH-Akt-GFP localization to the leading edge (Figure 5D). We next subjected the chemotaxing cells to an abrupt reversal in the direction of the gradient, as we did in earlier experiments. When control cells were subjected to gradient reversal, the majority executed a U-turn, and PH-Akt-GFP staining was restricted to the front throughout the turn (Figure 5D; Supplementary Material, Supplementary Video 7). In contrast, in cholesterol-depleted cells that reversed their polarity, PH-Akt-GFP staining appeared at the former rear before the formation of a new pseudopod (Figure 5D; Supplementary Material, Supplementary Video 8), whereas the membrane staining at the former front decreased. This indicates that plasma membrane cholesterol is critical for limiting D3-PI synthesis to a single area of the membrane in cells responding to changes in the direction of a chemoattractant gradient.

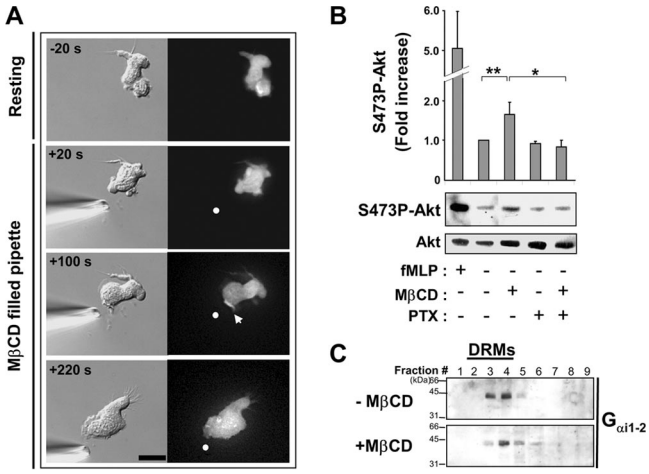

Figure 6. Cholesterol depletion induces pseudopod formation in a PI3-K- and G_i-dependent manner. (A) DIC and fluorescence images showing the response of a PH-Akt-GFP-expressing cell to cholesterol depletion using a micropipette filled with 2.5 mM MβCD (Supplementary Video 8). The arrowhead indicates PH-Akt-GFP membrane staining, and the dot indicates the position of the micropipette tip. Scale bar, 10 μm. (B) Measurement of Ser473P-Akt levels by Western blotting and densitometry analysis in the absence or presence of MβCD (2.5 mM, 3 min), pertussis toxin (PTX; 1 μg/ml, overnight), and fMLP (1 μM, 1 min). Akt levels in each sample were also measured by Western blotting to provide an input control. The graph represents results from densitometry analysis expressed as the fold increase compared with control resting conditions (mean $\pm$ SD for 5 separate experiments). Differences between resting versus MβCD-treated (** $p < 0.01$), and MβCD- versus MβCD/PTX-treated cells (* $p < 0.05$), were statistically significant according to the Student's *t*-test. (C) Distribution of $G_{\alpha i1-2}$ across fractions of sucrose density gradient loaded with lysates from control and MβCD-treated cells, revealed by Western blotting using an anti-$G_{\alpha i1-2}$ antibody.

Cholesterol Directly Modulates the Activation of the G_i/PI3-K Pathway

We next sought to determine how cholesterol participates in limiting D3-PI accumulation and pseudopod formation to a single area of the plasma membrane under chemokinesis and chemotaxis conditions. Because cholesterol depletion caused modest activation of PI3-K in the absence of fMLP (Figure 5A) and because PI3-K activation normally correlates with the development of a pseudopod, we asked whether cholesterol depletion could trigger pseudopod formation. We exposed PH-Akt-GFP expressing dHL-60 cells to a gradient of MβCD diffusing from a micropipette in the absence of fMLP to generate a gradient of cholesterol-depleting conditions across the plasma membrane of the cell. The parameters used to create the gradient of MβCD were identical to those used to generate a gradient of fMLP and were similar to those previously described for depleting cholesterol from one surface of a growth cone (Guirland *et al.,* 2004). After only 1.5 min of exposure to the MβCD gradient, most cells (80%, n = 15) developed a pseudopod facing the micropipette-tip, despite the fact that no chemoattractant was present (Figure 6A). MβCD-induced pseudopod formation was accompanied by local D3-PI accumulation as assessed by transient PH-Akt-GFP recruitment to the pseudopod (Figure 6A; Supplementary Material, Supplementary Video 9). This asymmetrical response was likely the result of a difference in the levels of cholesterol depletion from one side of the cell to the other, because cholesterol depletion by uniform MβCD treatment induced transient PH-Akt-GFP recruitment and membrane ruffling around the entire cell periphery rather than at a single area on the surface (unpublished data).

The fact that pseudopod formation was induced by cholesterol depletion allowed us to examine whether cholesterol directly modulates the function of G_i and PI3-K, which normally promote pseudopod formation downstream of the activated fMLP receptor. In agreement with the effect of cholesterol depletion on PI3-K activity, we found that MβCD-induced pseudopod formation was inhibited by wortmannin (Supplementary Material, Supplementary Video 9; n = 12), indicating a dependence on PI3-K activation. Similarly, MβCD-induced pseudopod formation (Supplementary Material, Supplementary Video 9) and Akt phosphorylation (Figure 6B) were prevented in cells treated with the G_i inhibitor pertussis toxin (PTX; n = 12; Supplementary Material, Supplementary Video 9), indicating a dependence on G_i activation. This suggests a pathway in which cholesterol directly modulates the activity of G_i, which in turn affects PI3-K activity. In support of this hypothesis, we observed that a large fraction of the alpha subunit of G_{i1-2} was enriched in cholesterol-rich DRMs isolated from dHL-60 cells (Figure 6C), in keeping with previous reports (Nebl *et al.,* 2002; Foster *et al.,* 2003). Moreover, cholesterol depletion diminished the amount of $G_{\alpha i}$ recov-

ered with DRMs (Figure 6C). These observations suggest that a cholesterol-dependent membrane environment directly modulates G_i function, which affects the localization of PI3-K activation, and indirectly affects RhoA activation via a negative feedback mechanism.

DISCUSSION

Neutrophil polarization and migration require the asymmetrical function of distinct signaling pathways and cytoskeletal assemblies at the front and rear of the cell. The development of cellular asymmetry has been hypothesized to involve the formation of distinct plasma membrane domains at the front and rear containing different lipid and protein compositions. Cholesterol is known to promote the formation of discrete membrane domains, and it has been shown to play an essential role in neutrophil polarization and migration. However, little is known about its mechanistic role in these processes. Using controlled conditions for cholesterol depletion, we show that cholesterol plays an essential function in organizing the plasma membrane into domains that enable the local activation of distinct signaling pathways at the poles of the cell.

Cholesterol Is Critical for Polarization and Uropod Function

Cholesterol has been shown to be essential for polarization and migration of neutrophils (Pierini *et al.*, 2003) and dHL-60 cells (Gomez-Mouton *et al.*, 2004; Niggli *et al.*, 2004), as well as fibroblasts (Manes *et al.*, 1999), T-lymphocytes (Gomez-Mouton *et al.*, 2001), and endothelial cells (Vasanji *et al.*, 2004). Our results support this broad conclusion. However, our observations reveal for the first time a mechanistic explanation for the function of cholesterol in polarization and migration.

We found that cholesterol is critical in dHL-60 cells for self-polarization in response to uniform chemoattractant stimulation. Cells subjected to cholesterol depletion and subsequently stimulated with uniform fMLP formed pseudopods, but most were unable to form a single stable pseudopod or to maintain stable polarity. Many cells formed multiple protruding pseudopods, either simultaneously or in rapid succession. We also found that cholesterol is critical for dHL-60 cell chemotaxis in response to an fMLP gradient. Under chemotaxis conditions, cells subjected to cholesterol depletion polarized and formed a single stable pseudopod, but did not migrate efficiently. These observations contrast with published findings, which report complete inhibition of pseudopod formation in response to uniform fMLP (Pierini *et al.*, 2003), and complete inhibition of polarization and migration in response to an fMLP gradient (Gomez-Mouton *et al.*, 2004). This discrepancy might be due to differences in cholesterol depletion conditions. For example, in agreement with our observations, others have reported that moderate cholesterol depletion did not prevent transient polarization of dHL-60 cells stimulated with uniform fMLP, whereas conditions leading to more profound depletion completely inhibited polarization (Niggli *et al.*, 2004). In addition, the discrepancy may be attributed to the fact that polarization and migration processes in different cell types might exhibit different sensitivities to cholesterol depletion. Indeed, after similar MβCD-treatments, membrane extension and ruffling were abolished in polymorphonuclear neutrophils (Pierini *et al.*, 2003) but still observed in dHL-60 cells (Gomez-Mouton *et al.*, 2004; this study), macrophages (Gatfield and Pieters, 2000), and MCF-7 cells (Manes *et al.*, 1999).

By carefully examining the behavior of single cells under moderate depletion conditions, we were able to determine which aspects of neutrophil polarization and migration were dependent on membrane cholesterol. In cholesterol-depleted cells that polarized, the velocity of pseudopod extension was unaffected, but uropod retraction was almost completely abolished. Moreover, the stability of the uropod was disrupted, as cells readily reversed polarity and converted their uropod into a pseudopod upon inversion of the fMLP gradient. These observations indicate that cholesterol is essential for promoting a balance between pseudopod-promoting and uropod-promoting pathways that allows uropod formation.

Cholesterol Facilitates Activation of the RhoA-dependent Rear Pathway

Interestingly, the behaviors caused by cholesterol depletion in dHL-60 cells—formation of multiple protrusions in response to uniform fMLP and failure to form a functional and stable uropod in response to an fMLP gradient—are similar to those caused by inactivating RhoA, MLC-K, and myosin II in neutrophils (Eddy *et al.*, 2002), dHL-60 cells (Xu *et al.*, 2003), and other cell types (Worthylake *et al.*, 2001). This suggests that cholesterol plays a critical role in promoting activation of the RhoA-dependent rear pathway. In support of this idea, we observed that cholesterol depletion inhibited RhoA activation and disrupted RhoA localization in response to uniform fMLP. Importantly, we showed that the effect of cholesterol depletion on RhoA activity is an indirect consequence of an effect on G_i signaling, as activation of the RhoA-pathway is restored in cholesterol-depleted treated cells when G_i is inhibited by PTX. This supports the idea that cholesterol indirectly promotes the activation of the RhoA-pathway by suppressing activation of the G_i/PI3-K pathway, which in neutrophils has been proposed to exert negative feedback on RhoA signaling (Weiner *et al.*, 2002; Xu *et al.*, 2003).

Cholesterol Participates in Restricting the Lateral Distribution of D3-PI Synthesis Sites

After stimulation of neutrophils with uniform fMLP, D3-PIs, and F-actin initially accumulate uniformly around the plasma membrane, and as cells polarize they become focused in the pseudopod (Servant *et al.*, 2000). We found that cholesterol depletion did not interfere with the initial, uniform accumulation of D3-PIs and F-actin in response to fMLP, in agreement with previous observations (Gomez-Mouton *et al.*, 2004). We also found that cholesterol depletion did not inhibit PI3-K activation, in contrast to previous reports that PI3-K activation was partially inhibited by cholesterol depletion in dHL-60 cells (Niggli *et al.*, 2004) and completely inhibited in platelets (Bodin *et al.*, 2001) and Vero cells (Peres *et al.*, 2003). Discrepancies between our observations and those in previous studies may be due to different depletion conditions, as discussed above, or to the involvement of distinct PI3-K isoforms in different cell types.

Intriguingly, although cholesterol was not critical for D3-PI synthesis in dHL-60 cells, it was essential for restricting D3-PI accumulation to the pseudopod upon uniform fMLP stimulation, or upon sudden changes in the orientation of an fMLP gradient. These observations provide a molecular explanation for the inability of cholesterol-depleted cells to establish or maintain their polarity. Indeed, if D3-PIs are not confined to a single membrane area, actin polymerization will be stimulated at multiple sites, leading to the formation of multiple pseudopods. Accumulation of D3-PIs and F-actin has also been proposed to exert negative

feedback on the RhoA pathway and uropod formation (Xu *et al.*, 2003), as discussed above.

How does cholesterol participate in restricting D3-PIs accumulation to the pseudopod? We observed that cholesterol depletion from resting cells was itself sufficient to induce PI3-K activation, D3-PI synthesis, and pseudopod formation. This agrees with the published observation that cholesterol depletion has a stimulatory effect on actin polymerization in neutrophils (Fessler *et al.*, 2004). PI3-K activation, D3-PI accumulation, and pseudopod formation were blocked by pertussis toxin, indicating that these events required the activation of G_i. Thus cholesterol contributes to a membrane environment that dampens G_i activity, which in turn suppresses PI3-K activity and D3-PI production. One mechanism by which cholesterol may regulate G_i is by modulating its interactions with activating proteins such as the fMLP receptor. This idea is supported by the observation that $G_{\alpha i}$ cofractionates with cholesterol-rich DRMs isolated from dHL-60 cells (this study), neutrophils (Nebl *et al.*, 2002), and other cell types (Foster *et al.*, 2003). In contrast, the inactive fMLP receptor partitions into different membrane domains (Jesaitis *et al.*, 1988; Jesaitis *et al.*, 1989). However, upon activation, it translocates into cholesterol-rich microdomains (Xue *et al.*, 2004). Differential partitioning of the fMLP receptor and G_i may be important for regulating their interaction at the front and rear of cells. Depletion of cholesterol may promote inappropriate G_i activation at the rear, tipping the balance in favor of pseudopod formation. This hypothesis is supported by our observation that in polarized cells exposed to MβCD, abnormal ruffling activity starts near the rear.

In addition to G_i and PI3-K, cholesterol may also influence the activity of other signaling proteins. One candidate is the D3-PI 3-phosphatase PTEN, which is localized to the rear in polarized *Dictyostelium* cells, where it prevents D3-PI accumulation (Iijima *et al.*, 2004). In neutrophils, whether PTEN is exclusively localized at the uropod is a matter of debate (Li *et al.*, 2003; Xu *et al.*, 2003; Li *et al.*, 2005). Our results suggest that PTEN is excluded from the pseudopod and uniformly distributed in the remainder of the cell (S. Bodin and M.D. Welch, unpublished observations). However, no changes in PTEN distribution were detected after cholesterol depletion. Thus, if cholesterol depletion affects PTEN, it is more likely to do so at the level of activity, and not localization.

Cholesterol may also influence properties of the membrane, such as fluidity, that impact signaling pathways as well as cytoskeletal functions. As suggested by previous studies, cholesterol might be concentrated in the pseudopod of polarized migrating cells (Gomez-Mouton *et al.*, 2004; Vasanji *et al.*, 2004). An enrichment of cholesterol at the leading edge may enhance membrane microviscosity (Vasanji *et al.*, 2004), which could in turn facilitate the assembly of signaling complexes involved in pseudopod protrusion or help restrict the lateral mobility of D3-PIs and the proteins involved in their synthesis. Indeed, altering the composition of the membrane by the addition of exogenous lipids in a way that may alter parameters such as fluidity and curvature has been shown to influence PI3-K activity (Hubner *et al.*, 1998; Bettache *et al.*, 2003)

A Model for the Function of Cholesterol in Neutrophil Polarization and Migration

We propose a model for the role of cholesterol in neutrophil polarization and migration (Figure 7). In this model, cholesterol is critical for the formation of membrane domains that enable spatial segregation of key signaling pathways at the front and rear of cells. At the molecular level, cholesterol plays a key role in confining the activation of the G_i/PI3-K pathway to a single membrane area that defines the pseudopod. This may be accomplished by several mechanisms. Cholesterol may function to concentrate signaling proteins and inhibit D3-PI lateral diffusion in the pseudopod. Moreover, cholesterol may down-regulate the Gi/PI3-K pathway, inhibiting negative feedback on the RhoA pathway in the uropod. When cholesterol is depleted from cells, the G_i/PI3-K pathway is inappropriately activated and D3-PIs accumulate over the entire plasma membrane. This is coupled with a loss of polarity, the formation of multiple protrusions, and an inhibition of uropod function. Future work should focus on defining the global organization and distribution of major phospholipids in the plasma membrane and elucidating how these contribute to the spatial organization of signaling events and cytoskeletal elements during polarization and migration.

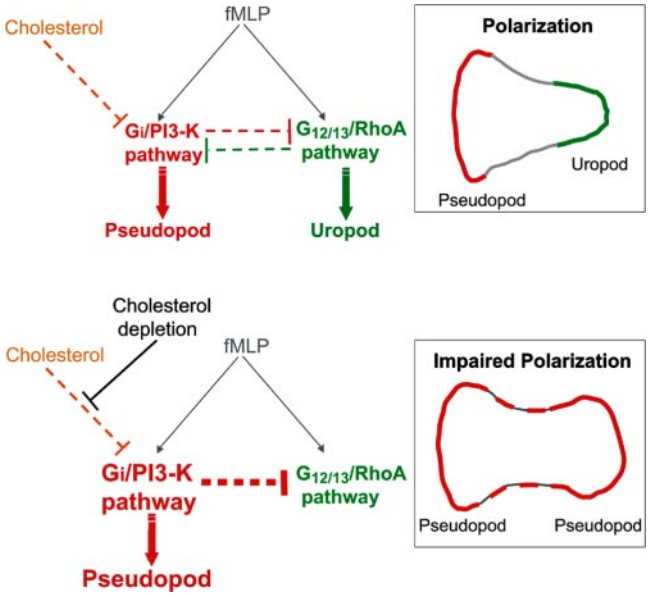

Figure 7. A model for the role of cholesterol in membrane organization during neutrophil polarization and migration. During polarization and migration (top diagram), activation of the fMLP-receptor at the front stimulates the G_i/PI3-K pathway (red), which promotes actin polymerization and protrusion. Receptor activation at the rear stimulates the $G_{12/13}$/RhoA pathway (green), which promotes actin-myosin contraction. These pathways segregate and are maintained at opposite poles of the cell in part via mutual negative feedback pathways (dotted red and green lines; Xu *et al.*, 2003). Cholesterol is critical for the formation of membrane domains that enable the spatial segregation of signaling pathways to the front and rear of cells. Cholesterol may directly influence the activation of signaling proteins involved in the G_i/PI3-K pathway and inhibit lateral diffusion of D3-PIs. Cholesterol may also down-regulate the G_i/PI3-K pathway in the uropod, inhibiting negative feedback on the RhoA pathway and promoting uropod formation. In response to cholesterol depletion by MβCD (bottom diagram), activation of the G_i/PI3-K pathway (red) is enhanced, leading to D3-PI accumulation over the entire plasma membrane, and to actin polymerization and the formation of multiple protrusions. This in turn enhances negative feedback on the RhoA pathway (green), inhibiting uropod function.

ACKNOWLEDGMENTS

We are grateful to Henry Bourne for the gift of PH-Akt-GFP expressing HL-60 cells, to Heidi Welch for the anti P-Rex1 antibody, to Steve Martin for the

GST-RBD construct, to Hai Tao He for technical advice on DRM isolation, and to Elizabeth Znameroski for technical assistance. We are indebted to Rebecca Heald, David Bilder, Robert Jeng, and Erin Goley for helpful comments on the manuscript, and to the Welch, Weis, and Heald labs for discussions throughout the course of this work. This work was supported by an Established Investigator Award from the American Heart Association to M.D.W. and by a postdoctoral fellowship from The Miller Institute for Basic Research in Sciences to S.B.

REFERENCES

Alblas, J., Ulfman, L., Hordijk, P., and Koenderman, L. (2001). Activation of RhoA and ROCK are essential for detachment of migrating leukocytes. Mol. Biol. Cell *12*, 2137–2145.

Benard, V., Bohl, B. P., and Bokoch, G. M. (1999). Characterization of rac and cdc42 activation in chemoattractant-stimulated human neutrophils using a novel assay for active GTPases. J. Biol. Chem. *274*, 13198–13204.

Bettache, N., Baisamy, L., Baghdiguian, S., Payrastre, B., Mangeat, P., and Bienvenue, A. (2003). Mechanical constraint imposed on plasma membrane through transverse phospholipid imbalance induces reversible actin polymerization via phosphoinositide 3-kinase activation. J. Cell Sci. *116*, 2277–2284.

Bodin, S., Giuriato, S., Ragab, J., Humbel, B. M., Viala, C., Vieu, C., Chap, H., and Payrastre, B. (2001). Production of phosphatidylinositol 3,4,5-trisphosphate and phosphatidic acid in platelet rafts: evidence for a critical role of cholesterol-enriched domains in human platelet activation. Biochemistry *40*, 15290–15299.

Dietrich, C., Bagatolli, L. A., Volovyk, Z. N., Thompson, N. L., Levi, M., Jacobson, K., and Gratton, E. (2001). Lipid rafts reconstituted in model membranes. Biophys. J. *80*, 1417–1428.

Drevot, P., Langlet, C., Guo, X. J., Bernard, A. M., Colard, O., Chauvin, J. P., Lasserre, R., and He, H. T. (2002). TCR signal initiation machinery is preassembled and activated in a subset of membrane rafts. EMBO J. *21*, 1899–1908.

Eddy, R. J., Pierini, L. M., Matsumura, F., and Maxfield, F. R. (2000). Ca2+-dependent myosin II activation is required for uropod retraction during neutrophil migration. J. Cell Sci. *113*(Pt 7), 1287–1298.

Eddy, R. J., Pierini, L. M., and Maxfield, F. R. (2002). Microtubule asymmetry during neutrophil polarization and migration. Mol. Biol. Cell *13*, 4470–4483.

Edidin, M. (2003). Lipids on the frontier: a century of cell-membrane bilayers. Nat. Rev. Mol. Cell. Biol. *4*, 414–418.

Fessler, M. B., Arndt, P. G., Frasch, S. C., Lieber, J. G., Johnson, C. A., Murphy, R. C., Nick, J. A., Bratton, D. L., Malcolm, K. C., and Worthen, G. S. (2004). Lipid rafts regulate lipopolysaccharide-induced activation of Cdc42 and inflammatory functions of the human neutrophil. J. Biol. Chem. *279*, 39989–39998.

Foster, L. J., De Hoog, C. L., and Mann, M. (2003). Unbiased quantitative proteomics of lipid rafts reveals high specificity for signaling factors. Proc. Natl. Acad. Sci. USA *100*, 5813–5818.

Friedrichson, T., and Kurzchalia, T. V. (1998). Microdomains of GPI-anchored proteins in living cells revealed by crosslinking. Nature *394*, 802–805.

Gatfield, J., and Pieters, J. (2000). Essential role for cholesterol in entry of mycobacteria into macrophages. Science *288*, 1647–1650.

Gomez-Mouton, C., Abad, J. L., Mira, E., Lacalle, R. A., Gallardo, E., Jimenez-Baranda, S., Illa, I., Bernad, A., Manes, S., and Martinez, A. C. (2001). Segregation of leading-edge and uropod components into specific lipid rafts during T cell polarization. Proc. Natl. Acad. Sci. USA *98*, 9642–9647.

Gomez-Mouton, C., Lacalle, R. A., Mira, E., Jimenez-Baranda, S., Barber, D. F., Carrera, A. C., Martinez, A. C., and Manes, S. (2004). Dynamic redistribution of raft domains as an organizing platform for signaling during cell chemotaxis. J. Cell Biol. *164*, 759–768.

Gousset, K., Wolkers, W. F., Tsvetkova, N. M., Oliver, A. E., Field, C. L., Walker, N. J., Crowe, J. H., and Tablin, F. (2002). Evidence for a physiological role for membrane rafts in human platelets. J. Cell Physiol. *190*, 117–128.

Guirland, C., Suzuki, S., Kojima, M., Lu, B., and Zheng, J. Q. (2004). Lipid rafts mediate chemotropic guidance of nerve growth cones. Neuron *42*, 51–62.

Hubner, S., Couvillon, A. D., Kas, J. A., Bankaitis, V. A., Vegners, R., Carpenter, C. L., and Janmey, P. A. (1998). Enhancement of phosphoinositide 3-kinase (PI 3-kinase) activity by membrane curvature and inositol-phospholipid-binding peptides. Eur. J. Biochem. *258*, 846–853.

Iijima, M., Huang, Y. E., Luo, H. R., Vazquez, F., and Devreotes, P. N. (2004). Novel mechanism of PTEN regulation by its phosphatidylinositol 4,5-bisphosphate binding motif is critical for chemotaxis. J. Biol. Chem. *279*, 16606–16613.

Ilangumaran, S., Briol, A., and Hoessli, D. C. (1998). CD44 selectively associates with active Src family protein tyrosine kinases Lck and Fyn in glycosphingolipid-rich plasma membrane domains of human peripheral blood lymphocytes. Blood *91*, 3901–3908.

Ilangumaran, S., and Hoessli, D. C. (1998). Effects of cholesterol depletion by cyclodextrin on the sphingolipid microdomains of the plasma membrane. Biochem. J. *335*, 433–440.

Jesaitis, A. J., Bokoch, G. M., Tolley, J. O., and Allen, R. A. (1988). Lateral segregation of neutrophil chemotactic receptors into actin- and fodrin-rich plasma membrane microdomains depleted in guanyl nucleotide regulatory proteins. J. Cell Biol. *107*, 921–928.

Jesaitis, A. J., Tolley, J. O., Bokoch, G. M., and Allen, R. A. (1989). Regulation of chemoattractant receptor interaction with transducing proteins by organizational control in the plasma membrane of human neutrophils. J. Cell Biol. *109*, 2783–2790.

Klein, U., Gimpl, G., and Fahrenholz, F. (1995). Alteration of the myometrial plasma membrane cholesterol content with beta-cyclodextrin modulates the binding affinity of the oxytocin receptor. Biochemistry *34*, 13784–13793.

Li, Z. *et al.* (2005). Regulation of PTEN by Rho small GTPases. Nat. Cell Biol. *7*, 399–404.

Li, Z. *et al.* (2003). Directional sensing requires G beta gamma-mediated PAK1 and PIX alpha-dependent activation of Cdc42. Cell *114*, 215–227.

Li, Z., Jiang, H., Xie, W., Zhang, Z., Smrcka, A. V., and Wu, D. (2000). Roles of PLC-beta2 and -beta3 and PI3Kgamma in chemoattractant-mediated signal transduction. Science *287*, 1046–1049.

Manes, S., Mira, E., Gomez-Mouton, C., Lacalle, R. A., Keller, P., Labrador, J. P., and Martinez, A. C. (1999). Membrane raft microdomains mediate front-rear polarity in migrating cells. EMBO J. *18*, 6211–6220.

Millan, J., Montoya, M. C., Sancho, D., Sanchez-Madrid, F., and Alonso, M. A. (2002). Lipid rafts mediate biosynthetic transport to the T lymphocyte uropod subdomain and are necessary for uropod integrity and function. Blood *99*, 978–984.

Nebl, T., Pestonjamasp, K. N., Leszyk, J. D., Crowley, J. L., Oh, S. W., and Luna, E. J. (2002). Proteomic analysis of a detergent-resistant membrane skeleton from neutrophil plasma membranes. J. Biol. Chem. *277*, 43399–43409.

Niggli, V. (1999). Rho-kinase in human neutrophils: a role in signalling for myosin light chain phosphorylation and cell migration. FEBS Lett. *445*, 69–72.

Niggli, V. (2000). A membrane-permeant ester of phosphatidylinositol 3,4,5-trisphosphate (PIP(3)) is an activator of human neutrophil migration. FEBS Lett. *473*, 217–221.

Niggli, V., and Keller, H. (1997). The phosphatidylinositol 3-kinase inhibitor wortmannin markedly reduces chemotactic peptide-induced locomotion and increases in cytoskeletal actin in human neutrophils. Eur. J. Pharmacol. *335*, 43–52.

Niggli, V., Meszaros, A. V., Oppliger, C., and Tornay, S. (2004). Impact of cholesterol depletion on shape changes, actin reorganization, and signal transduction in neutrophil-like HL-60 cells. Exp. Cell. Res. *296*, 358–368.

Pardo, M., and Nurse, P. (2003). Equatorial retention of the contractile actin ring by microtubules during cytokinesis. Science *300*, 1569–1574.

Parent, C. A. (2004). Making all the right moves: chemotaxis in neutrophils and *Dictyostelium*. Curr. Opin. Cell Biol. *16*, 4–13.

Peres, C., Yart, A., Perret, B., Salles, J. P., and Raynal, P. (2003). Modulation of phosphoinositide 3-kinase activation by cholesterol level suggests a novel positive role for lipid rafts in lysophosphatidic acid signalling. FEBS Lett. *534*, 164–168.

Pierini, L. M., Eddy, R. J., Fuortes, M., Seveau, S., Casulo, C., and Maxfield, F. R. (2003). Membrane lipid organization is critical for human neutrophil polarization. J. Biol. Chem. *278*, 10831–10841.

Pizzo, P., Giurisato, E., Tassi, M., Benedetti, A., Pozzan, T., and Viola, A. (2002). Lipid rafts and T cell receptor signaling: a critical re-evaluation. Eur. J. Immunol. *32*, 3082–3091.

Ren, X. D., Kiosses, W. B., and Schwartz, M. A. (1999). Regulation of the small GTP-binding protein Rho by cell adhesion and the cytoskeleton. EMBO J. *18*, 578–585.

Sasaki, T. *et al.* (2000). Function of PI3Kgamma in thymocyte development, T cell activation, and neutrophil migration. Science *287*, 1040–1046.

Servant, G., Weiner, O. D., Herzmark, P., Balla, T., Sedat, J. W., and Bourne, H. R. (2000). Polarization of chemoattractant receptor signaling during neutrophil chemotaxis. Science *287*, 1037–1040.

Seveau, S., Eddy, R. J., Maxfield, F. R., and Pierini, L. M. (2001). Cytoskeleton-dependent membrane domain segregation during neutrophil polarization. Mol. Biol. Cell *12*, 3550–3562.

Shefcyk, J., Yassin, R., Volpi, M., Molski, T. F., Naccache, P. H., Munoz, J. J., Becker, E. L., Feinstein, M. B., and Sha'afi, R. I. (1985). Pertussis but not cholera toxin inhibits the stimulated increase in actin association with the cytoskeleton in rabbit neutrophils: role of the "G proteins" in stimulus-response coupling. Biochem. Biophys. Res. Commun. *126*, 1174–1181.

Simons, K., and Ikonen, E. (1997). Functional rafts in cell membranes. Nature *387*, 569–572.

Singer, S. J., and Nicolson, G. L. (1972). The fluid mosaic model of the structure of cell membranes. Science *175*, 720–731.

Srinivasan, S., Wang, F., Glavas, S., Ott, A., Hofmann, F., Aktories, K., Kalman, D., and Bourne, H. R. (2003). Rac and Cdc42 play distinct roles in regulating PI(3,4,5)P3 and polarity during neutrophil chemotaxis. J. Cell Biol. *160*, 375–385.

Vasanji, A., Ghosh, P. K., Graham, L. M., Eppell, S. J., and Fox, P. L. (2004). Polarization of plasma membrane microviscosity during endothelial cell migration. Dev. Cell *6*, 29–41.

Wallace, P. J., Wersto, R. P., Packman, C. H., and Lichtman, M. A. (1984). Chemotactic peptide-induced changes in neutrophil actin conformation. J. Cell Biol. *99*, 1060–1065.

Wang, F., Herzmark, P., Weiner, O. D., Srinivasan, S., Servant, G., and Bourne, H. R. (2002). Lipid products of PI(3)Ks maintain persistent cell polarity and directed motility in neutrophils. Nat. Cell Biol. *4*, 513–518.

Weiner, O. D., Neilsen, P. O., Prestwich, G. D., Kirschner, M. W., Cantley, L. C., and Bourne, H. R. (2002). A PtdInsP(3)- and Rho GTPase-mediated positive feedback loop regulates neutrophil polarity. Nat. Cell Biol. *4*, 509–513.

Welch, H. C., Coadwell, W. J., Ellson, C. D., Ferguson, G. J., Andrews, S. R., Erdjument-Bromage, H., Tempst, P., Hawkins, P. T., and Stephens, L. R. (2002). P-Rex1, a PtdIns(3,4,5)P3- and Gbetagamma-regulated guanine-nucleotide exchange factor for Rac. Cell *108*, 809–821.

Worthylake, R. A., Lemoine, S., Watson, J. M., and Burridge, K. (2001). RhoA is required for monocyte tail retraction during transendothelial migration. J. Cell Biol. *154*, 147–160.

Xu, J., Wang, F., Van Keymeulen, A., Herzmark, P., Straight, A., Kelly, K., Takuwa, Y., Sugimoto, N., Mitchison, T., and Bourne, H. R. (2003). Divergent signals and cytoskeletal assemblies regulate self-organizing polarity in neutrophils. Cell *114*, 201–214.

Xu, X., and London, E. (2000). The effect of sterol structure on membrane lipid domains reveals how cholesterol can induce lipid domain formation. Biochemistry *39*, 843–849.

Xue, M., Vines, C. M., Buranda, T., Cimino, D. F., Bennett, T. A., and Prossnitz, E. R. (2004). N-formyl peptide receptors cluster in an active Raft-associated state prior to phosphorylation. J. Biol. Chem. *279*, 45175–45184.

Zigmond, S. H., Levitsky, H. I., and Kreel, B. J. (1981). Cell polarity: an examination of its behavioral expression and its consequences for polymorphonuclear leukocyte chemotaxis. J. Cell Biol. *89*, 585–592.

Zurzolo, C., van Meer, G., and Mayor, S. (2003). The order of rafts. Conference on microdomains, lipid rafts and caveolae. EMBO Rep. *4*, 1117–1121.